Heterodimerization of a Functional $GABA_B$ Receptor Is Mediated by Parallel Coiled-Coil α-Helices†

Richard A. Kammerer,‡ Sabine Frank,‡ Therese Schulthess, Ruth Landwehr, Ariel Lustig, and Jürgen Engel*

Department of Biophysical Chemistry, Biozentrum, University of Basel, Klingelbergstrasse 70, CH-4056 Basel, Switzerland

Received May 4, 1999; Revised Manuscript Received July 22, 1999

ABSTRACT: A detailed understanding of $GABA_B$ receptor assembly is an important issue in view of its role as attractive target for treatment of epilepsy, anxiety, depression, cognitive defects, and nociceptive disorders. Heteromerization of $GABA_B$-R1 and $GABA_B$-R2 subunits is a prerequisite for the formation of a functional $GABA_B$ receptor. Each individual subunit contains one stretch of ∼30 amino acid residues within its intracellular C-terminal domain that mediates heteromer formation. To investigate the mechanism of the $GABA_B$-R1/$GABA_B$-R2 interaction and to assess the subunit stoichiometry of the complex, recombinant polypeptide chain fragments containing the heteromerization site were produced by heterologous gene expression in *Escherichia coli*. When mixed in equimolar amounts, these peptides preferentially formed parallel coiled-coil heterodimers under physiological buffer conditions. This demonstrates that the short C-terminal regions are sufficient to determine the specificity of interaction between $GABA_B$ receptor subunits. In contrast, isolated $GABA_B$-R1 peptides folded into relatively unstable homodimers, whereas $GABA_B$-R2 peptides were largely unstructured. Together with the data reported in the literature, the results presented here indicate that the functional $GABA_B$ receptor is a heterodimer assembled by parallel coiled-coil α-helices.

γ-Aminobutyric acid (GABA)[1] is the main inhibitory neurotransmitter in the vertebrate central nervous system, where it exerts its effects through ionotropic ($GABA_A$/$GABA_C$) and metabotropic ($GABA_B$) receptor systems (*1*−*4*). In contrast to type A and C receptors, which mediate fast inhibitory activity, $GABA_B$ receptors produce slow, prolonged synaptic inhibition through G protein-coupled second-messenger pathways (*2*, *3*). Via these signal transduction molecules, they regulate the release of neurotransmitters and the activity of ion channels and adenylyl cyclase (*3*).

Recently, two homologous genes encoding $GABA_B$ receptor isoforms, termed $GABA_B$-R1 and $GABA_B$-R2, have been cloned from man and rat (*5*−*11*). $GABA_B$-R1 exists in two splice variants (a and b) which differ in their N-termini (*5*). At the protein level, the two receptors share 35% identical residues (*6*−*10*). As expected, both proteins belong to the seven transmembrane, G protein-coupled receptor family. In particular, $GABA_B$ receptors are most closely related and similar in size to members of the metabotropic glutamate receptor family, which range from 872 to 1,203 amino acid residues (*5*, *12*−*15*). Members of this family contain an intracellular C-terminal domain, seven characteristic transmembrane spanning segments, and an extended N-terminal extracellular domain, which in case of the two $GABA_B$ receptors is N-glycosylated. $GABA_B$-R1 and $GABA_B$-R2 mRNAs are expressed only in the brain where they are very abundant and show considerable colocalization as revealed by in situ hybridization (*6*, *8*−*11*). Importantly, $GABA_B$-R1a, $GABA_B$-R1b, and $GABA_B$-R2, when expressed individually, show functional differences to endogenous $GABA_B$ receptors (*5*−*11*). In particular, neither $GABA_B$-R1 nor $GABA_B$-R2 alone activate Kir3- and GIRK-type potassium channels (*6*−*11*). Furthermore, $GABA_B$-R1a fails to reach the cell surface when expressed by itself in heterologous systems and is retained in the endoplasmatic reticulum (*16*). Thus, coexpression of $GABA_B$-R1 and $GABA_B$-R2 appears to be a prerequisite for the formation of a functional high affinity $GABA_B$ receptor (*6*−*11*, *16*).

Moreover, it has recently been demonstrated that $GABA_B$-R1 and $GABA_B$-R2 interact via their intracellular domains to form heterodimers or larger oligomers (*7*, *9*). On the basis of this observation, it has been speculated that this heterotypic interaction is mediated by coiled-coil α-helices (*7*). The α-helical coiled coil is probably the most widespread subunit oligomerization motif found in proteins (*17*−*20*). This type of protein structure consists of two to five amphipathic α-helices that "coil" around each other in a left-handed supertwist (*21*−*25*). The sequences of coiled coils are characterized by a heptad repeat of seven residues denoted **a**−**g**, with a 3,4-hydrophobic repeat of mostly apolar amino acids at positions **a** and **d** (*26*, *27*). Interactions between the core residues at **a** and **d** and its two flanking positions, **e**

† This work was supported by the Swiss National Science Foundation (Grant 31-49281.96 to J. E.).

* To whom correspondence should be addressed. Jürgen Engel, Department of Biophysical Chemistry, Biozentrum, University of Basel, Klingelbergstrasse 70, CH-4056 Basel, Switzerland. Telephone: +41 61 267-2250. Fax: +41 61 267-2189. E-mail:engel@ubaclu.unibas.ch.

‡ These authors contributed equally to this study.

[1] Abbreviations: $[\theta]_{221}$, mean molar residue ellipticity at 221 nm; *A*, absorbance; CD, circular dichroism; GABA, γ-aminobutyric acid; $GABA_B$-R, B-type GABA receptor; GuHCl, guanidine hydrochloride; kDa, kilodaltons; PCR, polymerase chain reaction; SDS−PAGE, sodium dodecyl sulfate polyacrylamide gel electrophoresis; T_m, midpoint of thermal denaturation.

10.1021/bi991018t CCC: $18.00
Published on Web 09/14/1999

and **g**, determine the number of strands, the parallel or antiparallel orientation of the α-helices, and the homo- or heterotypic association of subunits into a coiled coil (for review see refs *17*, *18*).

A detailed understanding of $GABA_B$ receptor assembly is an important issue in view of its role as attractive target for treatment of epilepsy, anxiety, depression, cognitive defects, and nociceptive disorders (*28*−*30*). To investigate the mechanism of the interaction between $GABA_B$-R1 and $GABA_B$-R2 in detail, we have produced recombinant $GABA_B$ receptor polypeptide chain fragments, containing the putative coiled-coil domains in *Escherichia coli*. Subsequently, we have analyzed the structures of the individual and combined peptides by nondenaturing PAGE, Tricine/SDS−PAGE, circular dichroism (CD) spectroscopy, and analytical ultracentrifugation. We found that $GABA_B$-R1 and $GABA_B$-R2 polypeptide chain fragments specifically interact to form a parallel coiled-coil heterodimer under physiological conditions. Together, with the data reported in the literature (*7*, *9*), our results indicate that the functional $GABA_B$ receptor is a heterodimer assembled by parallel coiled-coil α-helices. Although isolated coiled-coil domains usually display the same subunit stoichiometry as the native protein, an aggregation of $GABA_B$ receptor heterodimers to higher order oligomers cannot be excluded by our approach.

EXPERIMENTAL PROCEDURES

Construction of Expression Plasmids. DNA fragments coding for amino acid residues Glu-865 to His-927 (designated $GABA_B$-R1p) and Glu-885 to Ser-918 ($GABA_B$-R1 cc) of $GABA_B$-R1a (*7*) and Ser-774 to Tyr-825 ($GABA_B$-R2p) and Thr-785 to Asp-818 ($GABA_B$-R2 cc) of $GABA_B$-R2 (*7*) were amplified by PCR from human adult brain cDNA (Clontech). Oligonucleotide primer sets were designed ($GABA_B$-R1p: p-5′ (5′-CCCGGATCCGAATGGCAGTCGGAGGCG-3′) and p-3′ (5′-CCCGAATTCTTATTAGTGGCGCCGGGAGCGGAG-3′); $GABA_B$-R1 cc: p-5′ (5′-CCCGGATCCGAGGAGAAGTCCCGGCTGTTG-3′) and p-3′ (5′-TCTCCCGAATTCTTATTAGCAACCACCAGACTGGAGTTGATGGCGCAG-3′); $GABA_B$-R2p: p-5′ (5′-CCCGGATCCACCTCGGTCACCAGTG-3′) and p-3′ (5′-CCCGAATTCTTATTAGTAGGTGGTCTTTTCTGGTGTG-3′); and $GABA_B$-R2 cc: p-5′ (5′-CCCGGATCCACATCCCGCCTGGAGGGCC-3′) and p-3′ (5′-TCTCCCGAATTCTTATTAGCAACCACCGTCCTGCAGCTGCATGGTGAC-3′)) to obtain a *Bam*H I site at the 5′ end and two translation stop signals (TAA) followed by an *Eco*R I site at the 3′ end of each construct. In addition, the linker sequence Gly−Gly−Cys was introduced at the C-terminal end of $GABA_B$-R1 cc and $GABA_B$-R2 cc. The amplified products were ligated into the *Bam*H I/*Eco*R I site of the bacterial expression vectors pPEP-T ($GABA_B$-R1p, $GABA_B$-R2p, and $GABA_B$-R2 cc)(*31*) and pHisTrx2 ($GABA_B$-R1 cc)-(*32*). PCR and DNA manipulations for cloning were performed according to standard protocols (*33*). Recombinant insert DNA was verified by Sanger dideoxy DNA sequencing.

Expression and Purification of Recombinant $GABA_B$ Receptor Polypeptide Chain Fragments. The *E. coli* JM109(DE3) host strain (Promega) was used for expression. Production and purification of 6xHis-tagged fusion proteins by immobilized metal affinity chromatography on Ni^{2+}-Sepharose (Novagen) was performed under native ($GABA_B$-R1 cc) or denaturing conditions ($GABA_B$-R1p, $GABA_B$-R2p, and $GABA_B$-R2 cc) as described in the manufacturer's instructions. Separation of recombinant $GABA_B$ receptor polypeptide chain fragments from the 6xHis-tagged carrier protein by thrombin cleavage was carried out as described by Kammerer et al. (*32*). $GABA_B$-R2p contains one additional N-terminal Gly residue, and $GABA_B$-R1p and $GABA_B$-R2 cc carry two additional residues, Gly and Ser, at their N-termini, which originated from the expression plasmids and are not part of the $GABA_B$ receptor coding sequences. Recombinant polypeptide chain fragments were analyzed in 10 mM sodium phosphate buffer (pH 7.0) supplemented with 150 mM sodium chloride. Concentrations of $GABA_B$-R1p, $GABA_B$-R2p, and 6xHisTrx-$GABA_B$-R1 cc were determined by Trp and/or Tyr absorption in 6 M GuHCl (*34*) and the concentration of $GABA_B$-R2 cc was estimated by the BCA assay (Pierce).

Gel Electrophoresis. Nondenaturing PAGE and Tricine/SDS-PAGE (*35*) were performed on 12 × 13-cm slab gels at 4 °C and room temperature, respectively. Proteins were visualized by staining with Coomassie Brilliant Blue R-250. Apparent molecular masses were obtained by comparison with low molecular mass markers (Amersham Pharmacia Biotech and Sigma).

CD Spectroscopy. CD spectra were acquired on a Jasco J720 spectropolarimeter. Far-ultraviolet spectra (200−250 nm) were measured in a 0.2-mm path length quartz cell and represent averages of 10 accumulations. Spectra were normalized for concentration and path length to obtain the mean molar residue ellipticity after subtraction of the buffer contribution. Helix content was calculated by the method of Chen et al. (*36*). Temperature scans were recorded on a Cary 61 spectropolarimeter equipped with a thermostated 1-mm path length quartz cell. Thermal stability was determined by monitoring the change in the mean molar residue ellipticity at a fixed wavelength of 221 nm, $[\theta]_{221}$, as a function of temperature. A scan rate of 1 °C/min was used for all experiments. Data analysis was performed with the Jasco (Japan Spectroscopic Co.), LABView (National Instruments), and Sigma Plot (Jandel Scientific) software packages.

Analytical Ultracentrifugation. Sedimentation equilibrium and sedimentation velocity experiments were performed on a Beckman Optima XL-A analytical ultracentrifuge equipped with 12-mm Epon double-sector cells in an An-60 Ti rotor. The recombinant $GABA_B$ receptor peptides were analyzed in 10 mM sodium phosphate buffer (pH 7.0) supplemented with 150 mM sodium chloride, and protein concentrations were adjusted to 0.2−0.4 mg/mL. Sedimentation velocity runs were performed at 20 °C at a rotor speed of 56 000 rpm, and sedimenting material was assayed by its absorbance at 234 or 278 nm. Sedimentation coefficients were corrected to standard conditions (water, 20 °C)(*37*). Sedimentation equilibrium scans were carried out at 22 000 to 38 000 rpm, depending on molecular mass. Average molecular masses were evaluated by using a floating baseline computer program to obtain the best linear fit of $\ln A$ versus r^2 where A is the absorbance and r the distance from the rotor center (*37*). A partial specific volume of 0.73 mL/g was used for all calculations.

RESULTS AND DISCUSSION

The distinctive, repetitive pattern of the heptad repeat provides a characteristic feature for the identification of coiled-coil regions from the primary sequence of a protein. Secondary structure analysis, using the COILS algorithm (version 2.2; *18*, *38*), which compares an amino acid sequence with sequences in a database of known two-stranded coiled coils, predicts with high probability coiled-coil stretches from residues Glu-317 to Phe-339 and Glu-885 to Ser-918 in human $GABA_B$-R1a (*7*) and residues Thr-785 to Asp-818 in $GABA_B$-R2 (*7*). For other regions of the $GABA_B$ receptor subunit sequences, a tendency to assume a putative coiled-coil conformation was not predictable. Interestingly, the last two predicted coiled-coil domains approximately correspond to the sites that have been mapped to mediate the interaction between $GABA_B$-R1 and $GABA_B$-R2 by the yeast two-hybrid system (*9*). Using this approach, an interaction was found between $GABA_B$-R1 and $GABA_B$-R2, but not among $GABA_B$-R1 molecules or $GABA_B$-R2 molecules, suggesting a heterotypic assembly of the two receptor subunits. Interaction between the C-termini of $GABA_B$-R1 and $GABA_B$-R2 has also been confirmed by glutathione S-transferase fusion proteins (*9*).

To understand the mechanism of the $GABA_B$ receptor subunit interaction and to address the stoichiometry of the complex, two recombinant peptides, $GABA_B$-R1p and $GABA_B$-R2p, were produced by heterologous gene expression in *E. coli* (Figure 1A; see Experimental Procedures). To distinguish the two by Tricine/SDS-PAGE and analytical ultracentrifugation, $GABA_B$-R1p and $GABA_B$-R2p were designed to differ in size. In addition, both peptides contain an aromatic Tyr or Trp residue for protein quantitation. The homogeneity of the affinity-purified $GABA_B$ receptor peptides was assessed by Tricine/SDS-PAGE. Single bands migrating with mobilities corresponding to their expected molecular masses were detected (Figure 1B).

CD spectroscopy was used to test for the secondary structure of the peptides. The far-ultraviolet CD spectrum recorded from $GABA_B$-R1p indicated a substantial amount of α-helicity at 5 °C (Figure 2A). However, the CD spectrum was characteristic for partial helix formation as evidenced by a shift of the minimum from 208 to 205 nm. In contrast, $GABA_B$-R2p was largely unfolded at 5 °C as revealed by its CD spectrum; typical for proteins in a random coil conformation, there is a pronounced minimum at 200 nm (Figure 2A). However, when mixed in equimolar amounts, the CD spectrum of the combined $GABA_B$-R1p and $GABA_B$-R2p peptides displayed a significant increase in α-helicity with characteristic minima at 208 and 222 nm (Figure 2A). The $[\theta]_{222}$ value of $-25\,000$ deg cm^2 dmol^{-1}, which indicates a degree of α-helicity of ∼60−70% for a 75 μM total peptide solution (*36*), is consistent with the predicted coiled-coil stretches in the two peptides. This suggests that the combined $GABA_B$ receptor peptides form a heterotypic α-helical coiled-coil structure, a conclusion which is further supported by the temperature-induced denaturation profile recorded from the mixture at 221 nm (Figure 2B). The thermal unfolding profile exhibited the sigmoid shape typical for coiled coils, implying a two-state transition. Accordingly, the profile was monophasic and reversible with >90% of the starting signal regained on cooling. As expected,

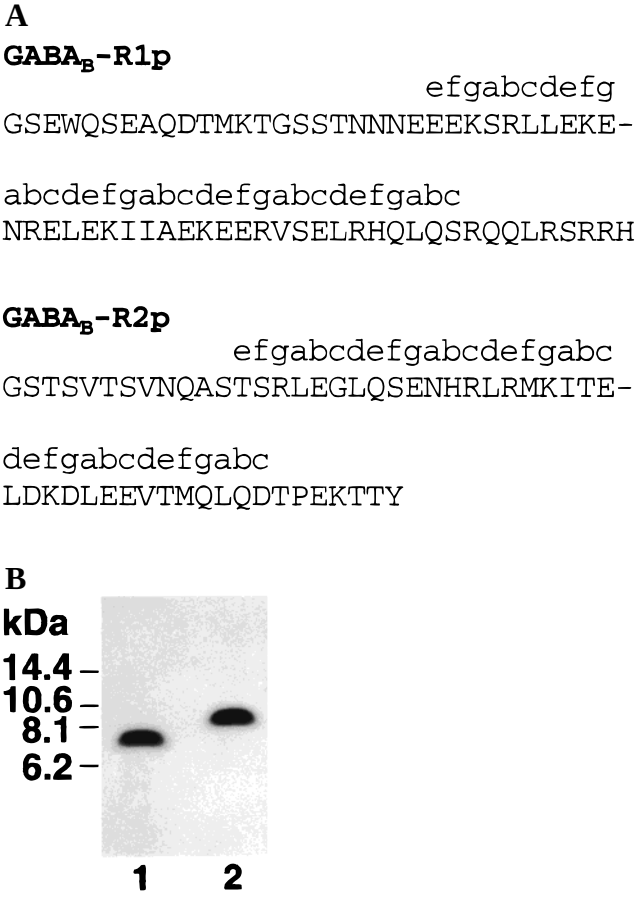

FIGURE 1: Design of $GABA_B$ receptor peptides. (*A*) Sequences of $GABA_B$-R1p and $GABA_B$-R2p, comprising residues Glu-865 to His-927 of $GABA_B$-R1a (*7*) and Ser-774 to Tyr-825 of $GABA_B$-R2 (*7*), with two (Gly−Ser) and one (Gly) additional N-terminal residues, respectively. Heptad positions of the predicted coiled-coil domains are indicated by lowercase letters. (*B*) Tricine/SDS-PAGE analysis under reducing conditions of recombinant $GABA_B$ receptor polypeptide chain fragments after affinity purification and thrombin cleavage. Lane 1, $GABA_B$-R1p; lane 2, $GABA_B$-R2p. ∼10 μg of peptide was loaded per lane. The migration of marker proteins is indicated.

concentration dependence of the midpoint of thermal unfolding (T_m) was observed for the mixed peptides (data not shown). At a total peptide concentration of 75 μM, the profile showed a T_m at 48 °C (Figure 2B). In contrast, the thermal melting profile recorded from $GABA_B$-R1p exhibited a broad, noncooperative transition, indicating partial unfolding of the peptide at low temperatures (Figure 2B). Consistent with its CD spectrum, $GABA_B$-R2p yielded no significant thermal unfolding profile (data not shown).

$GABA_B$-R1p and $GABA_B$-R2p peptides were designed to have net charges of −1 and −3, respectively. Accordingly, preferential heteromer formation of $GABA_B$ receptor peptides could also be demonstrated by nondenaturing PAGE (Figure 3). As nondenaturing gels separate on the basis of a combination of molecular mass, shape, and net charge of proteins, the faster electrophoretic mobility of the heterotypic complex (lane 2) relative to that of the $GABA_B$-R2p component (lane 3) can be understood in terms of formation of a compact structure, which is less resistant to migration in the electric field.

To determine the subunit stoichiometry of the $GABA_B$-R1/$GABA_B$-R2 heteromer, equimolar solutions of all peptide

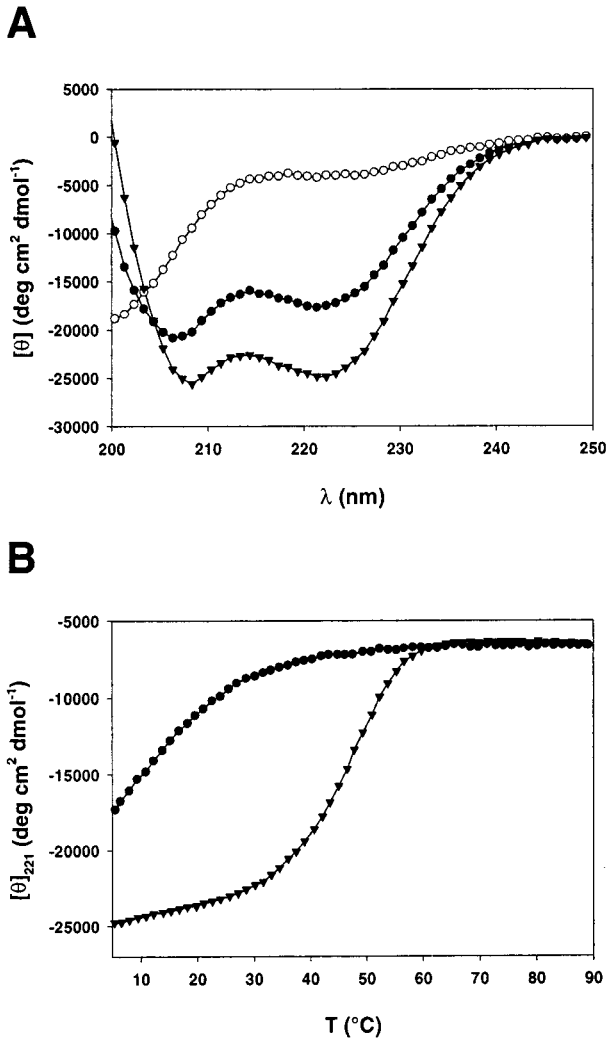

FIGURE 2: (*A*) Far-ultraviolet CD spectra recorded from $GABA_B$-R1p (●), $GABA_B$-R2p (○), and an equimolar mixture of both peptides (▼) at 5 °C. Peptide concentrations were 75 μM in 10 mM sodium phosphate (pH 7.0) containing 150 mM sodium chloride. A $[\theta]_{222}$ value of −25 000 deg cm^2 dmol^{-1} indicates that the mixture of both peptides is ∼60−70% helical. (*B*) Temperature induced unfolding profiles of $GABA_B$-R1p (●) and $GABA_B$-R1p/$GABA_B$-R2p (▼) monitored by the change of the CD signal at 221 nm. Only the mixed peptides exhibit a sigmoidal unfolding transition with a T_m of 48 °C. Peptide concentrations and buffer conditions were as above.

combinations were analyzed by analytical ultracentrifugation (Table 1). Sedimentation equilibrium yielded average molecular masses of 13.3, 14.1, and 15.0 kDa for the heterotypic $GABA_B$ receptor complex over a temperature range from 6 to 37 °C, which is consistent with the formation of a heterodimer (calculated molecular mass of 13.8 kDa). Furthermore, sedimentation velocity revealed a sedimentation coefficient of 1.28 S. This value is consistent with an elongated shape of a dimeric complex, because a globular protein of the same molecular mass would yield a sedimentation coefficient of 1.7 S and for globular monomeric $GABA_B$-R1p and $GABA_B$-R2p peptides $s_{20,w}$ values of 1.1 and 0.9 S, respectively, are predicted. Isolated $GABA_B$-R1p peptides appear to form a mixture of momomers and dimers at lower temperatures, which explains the broad, noncooperative thermal transition profile of the peptide. As expected from the peptide's thermal instability, an average molecular mass of 7.7 kDa corresponding to peptide monomers was

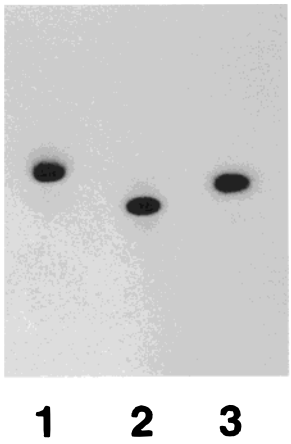

FIGURE 3: 10% nondenaturing PAGE performed at 4 °C indicating complex formation between $GABA_B$ receptor peptides. Lane 1, $GABA_B$-R1p; lane 2, $GABA_B$-R1p/$GABA_B$-R2p complex; lane 3, $GABA_B$-R2p. ∼5 μg of peptide was loaded per lane.

obtained at physiological body temperature (calculated molecular mass of 7.8 kDa). Over the entire temperature range analyzed, $GABA_B$-R2p exhibited molecular masses of 6.7, 7.2, and 7.5 kDa, indicative of the predominance of monomers (calculated molecular mass of 6 kDa).

Taken together, these findings demonstrate that, when mixed in equimolar amounts, $GABA_B$-R1p and $GABA_B$-R2p peptides preferentially form a heterodimeric coiled-coil.

Our results on the instability of $GABA_B$ receptor homodimers explain the lack of interaction observed among $GABA_B$-R1 or among $GABA_B$-R2 molecules in yeast two-hybrid screens (*7*, *9*). As the stability of a coiled coil is determined by interactions between residues in the hydrophobic interface, the instability of the $GABA_B$-R1p homodimer can be rationalized by the presence of Ser-888 and Asn-895 side chains at two heptad **a** positions and Lys-905 at a **d** position, all of which correspond to a violation of the 3,4-hydrophobic repeat. In particular, Lys residues are only very rarely found in **d** positions of dimers (*39*). The presence of a charged residue at a heptad **d** position is presumably a very efficient mechanism to destabilize the short homodimer. Similarly, replacement of Leu residues by Arg or Lys in the leucine zipper of GCN4 has been reported to significantly reduce the stability of this homodimeric coiled coil (*40*). In addition, the $GABA_B$-R1p homodimer is also disfavored by four repulsive electrostatic interchain i, i′+5 interactions between **e** and **g** residues (e.g., Glu-894/Glu-899′ and Arg-908/Arg-913′; residue i of chain 1 to residue i′+5 in chain 2; **g** to **e**′). Electrostatic interactions between these residues can occur because the side chains of residues at positions of **e**′ and **g** of the proceeding heptad are close to each other (*22*). It is likely that the close proximity of side chains of like charge at positions **e** and **g** of opposing $GABA_B$-R1 monomers disrupts the complementary packing at the dimer interface of the coiled coil, thus accounting for the instability of the $GABA_B$-R1 homodimers. A destabilization of homodimers due to the presence of unfavorable residues at the **a** and **d** positions as well as repulsive electrostatic interchain interactions has also been reported for the leucine zipper domains of the Fos and c-Myc transcription factors (*41*−*43*).

In contrast, the instability of $GABA_B$-R2p cannot be explained by the above factors alone. In fact, as the peptide

Table 1: Sedimentation Coefficients ($s_{20,w}$) and Average Molecular Masses of Recombinant $GABA_B$ Receptor Polypeptide Chain Fragments[a]

peptide	$s_{20,w}$(S)	molecular mass (kDa) observed	molecular mass (kDa) calculated[b]
$GABA_B$-R1p	0.98	13.3 (6 °C) 11.0 (20 °C) 7.7 (37 °C)	7.8
$GABA_B$-R2p	0.95	7.5 (6 °C) 7.2 (20 °C) 6.7 (37 °C)	6.0
$GABA_B$-R1p/$GABA_B$-R2p	1.28	15.0 (6 °C) 14.1 (20 °C) 13.3 (37 °C)	13.8
6xHisTrx-$GABA_B$-R1cc/$GABA_B$-R2cc	2.19	22.9 (20 °C)	22.8

[a] All peptides were analyzed in 10 mM sodium phosphate buffer (pH 7.0) containing 150 mM sodium chloride. [b] Molecular mass of the monomer or the heterodimer based on its amino acid sequence.

contains four attractive electrostatic **g** to **e′** interchain interactions and only one polar residue (Asn-795) in a heptad **a** position, one would rather expect a stable homotypic $GABA_B$-R2p coiled coil. Complete destabilization of $GABA_B$-R2p due to the presence of Gly-790 is also not likely, since a single Gly residue is found in the three-stranded coiled-coil domain of tenascin-C, which despite comprising only 3.5 heptad repeats is very stable (*32*). Therefore, the reasons for the instability of homotypic $GABA_B$-R2p coiled-coil structures remain elusive.

Recent evidence indicates that intrahelical i, i+3 and i, i+4 salt bridges favorably contribute to coiled-coil stability (*44*). By introduction of interactive combinations of surface salt bridges referred to as complex salt bridges into the GCN4 leucine zipper, Spek et al. (*44*) observed an increase in thermal stability of 22 °C of the mutant peptide relative to the wild-type. Interestingly, the number of possible i, i+3 and i, i+4 intrachain electrostatic interactions in the coiled-coil domains of $GABA_B$-R1 (10 attractive and 7 repulsive interactions) and $GABA_B$-R2 (5 attractive and 4 repulsive interactions) correlates with the relative peptide stabilities.

Notably, none of the repulsive electrostatic interchain interactions seen in $GABA_B$-R1p would be present in the parallel $GABA_B$-R1/$GABA_B$-R2 heterodimer. Likewise, relief of unfavorable electrostatic interactions in Fos and c-Myc leucine zipper homodimers appears to account for heterodimerization specificity of Jun/Fos and c-Myc/Max transcription factors (*41*−*43*, *45*−*47*). To probe the relative helix orientation in the $GABA_B$ receptor heterodimer, two additional peptides denoted $GABA_B$-R1 cc and $GABA_B$-R2 cc were generated. Both peptides exactly correspond to the predicted coiled-coil stretches and contain a C-terminal Gly−Gly−Cys linker sequence. In addition, to distinguish the two peptides on Tricine/SDS gels, $GABA_B$-R1 cc was fused to the C-terminus of 6xHis-tagged thioredoxin (*32*). As revealed by Tricine/SDS-PAGE analysis, specific formation of covalently linked heterodimers was observed after air oxidation of an equimolar mixture of the reduced peptides (Figure 4A, compare lanes 2 and 5). As expected, the single free Cys sulfhydryl group of the C-terminal Gly−Gly−Cys extension also produced disulfide-linked homodimers of individual 6xHis-$GABA_B$-R1 cc (lane 1) and $GABA_B$-R2 cc (lane 3) peptides. Sedimentation equilibrium of the disulfide-linked heterotypic complex yielded an average molecular mass of 22.9 kDa (Table 1), a value that is consistent with the formation of a heterodimer (calculated molecular mass of 22.8 kDa). The observation that the disulfide-linked $GABA_B$ receptor heterodimer did not aggregate into larger oligomers indicates that $GABA_B$-R1 cc and $GABA_B$-R2 cc peptides have a significant preference for a parallel alignment of their constituent helices (Figure 4B).

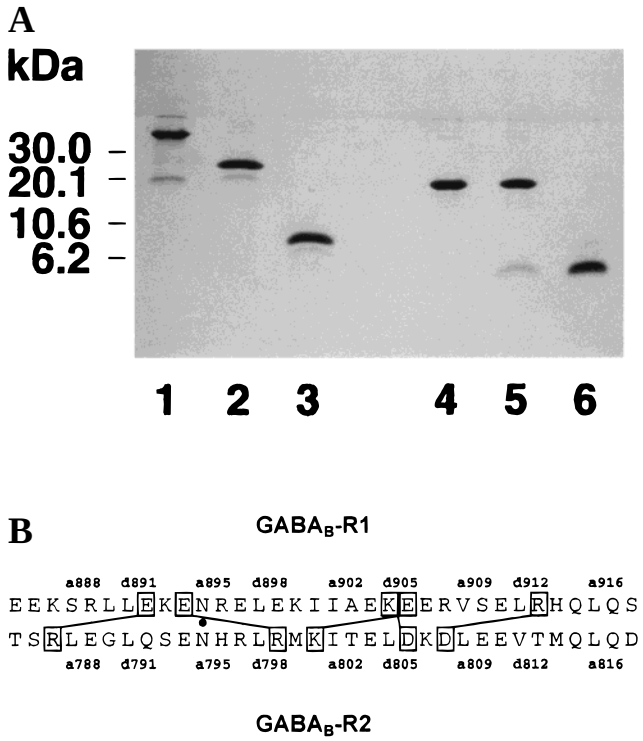

FIGURE 4: (*A*) Tricine/SDS-Page analysis of disulfide-linked peptide combinations under nonreducing (lanes 1−3) and reducing conditions (lanes 4−6) indicates formation of a parallel heterotypic $GABA_B$ receptor coiled-coil. Lanes 1 and 4, 6xHisTrx-$GABA_B$-R1 cc; lanes 2 and 5, 6xHisTrx-$GABA_B$-R1 cc/$GABA_B$-R2 cc; lanes 3 and 6, $GABA_B$-R2 cc. ~10 μg of peptide was loaded per lane. (*B*) Model of the $GABA_B$ receptor coiled-coil heterodimer with constituent α-helices arranged in parallel register. Residues that make putative electrostatic interactions between subunits are boxed and connected by lines. The dot indicates the buried, polar interaction between Asn residues at position **a** of the second heptad repeat. Heptad positions are indicated by lowercase letters and numbers refer to amino acid positions within $GABA_B$ receptor proteins. The coiled-coil domains of $GABA_B$-R1 and $GABA_B$-R2 subunits share 29% identical and 38% similar residues.

Together with the data reported in the literature (*7*, *9*), these results indicate that the functional $GABA_B$ receptor is a parallel heterodimer assembled by coiled-coil α-helices.

A likely determinant for parallel helix orientation and chain stoichiometry in the $GABA_B$ receptor heterodimer is the polar Asn residue at position **a** of the second heptad repeat present in both peptides (Figure 4B). It has been demonstrated that a hydrogen-bonded Asn−Asn buried polar interaction imparts structural uniqueness to the leucine zipper of GCN4 as well as to a synthetic heterodimeric coiled-coil derivative termed "Velcro" (*48*−*50*). Importantly, mutants, though they formed a more stable complex, did no longer fold into a unique structure (*48*, *49*) or were lacking a specific chain orientation (*50*). There exists a second, buried polar residue (Lys-905) at position **d** of the third heptad repeat in $GABA_B$-R1 cc (Figure 4B), which may also play a role in $GABA_B$ receptor heterodimer specificity. A similar situation is observed in the antiparallel seryl-tRNA synthetase coiled coil where Arg-54 at a **d** position interacts with Glu-74 in a **g′** position of the neighboring helix (*51*). As the analogous interaction is **a** to **e′** in a parallel coiled coil, there exists a possible interaction between Lys-905 and Asp-806 in the $GABA_B$ receptor heterodimer. In addition, the parallel heterodimer exhibits four favorable electrostatic **g** to **e′** interchain interactions (e.g., Arg-787/Glu-892′, Glu-894/Arg-799′, Lys-801/Glu-906′, and Asp-808/Arg-913′). It is generally accepted that relief of unfavorable electrostatic interactions in homodimers substantially contribute to heterodimerization specificity. However, the contribution of interhelical electrostatic **g** to **e′** interactions to coiled-coil stability is fiercely debated in the recent literature (*52*−*55*).

Finally, it has been demonstrated that the type of hydrophobic residue occupying the core positions can exert a major influence on oligomer specificity (*23*, *24*). Major roles in oligomer specification are played by Leu and Ile. Dimers were found to be favored by sequences enriched for Ile at the **a** sites and Leu at **d** (*23*). The preference for specific amino acids at the core positions of dimers can be explained in terms of a different packing geometry of side chains at the **a** and **d** positions (*22*). Consequently, Ile and Leu side chains can be best accommodated at **a** and **d** positions, respectively. Notably, the distribution of Ile and Leu residues at the a and d positions of the $GABA_B$-R1 and $GABA_B$-R2 coiled-coil domains is consistent with a dimeric structure of the complex (Figure 4B).

Taken together, our findings demonstrate that the interaction between $GABA_B$-R1 and $GABA_B$-R2 subunits is mediated by a parallel heterodimeric coiled coil. On the basis of the fact that isolated coiled-coil domains usually display the same subunit stoichiometry as the native protein, we anticipate the structure of the functional $GABA_B$ receptor to be that of a parallel heterodimer. However, limited by our approach using polypeptide chain fragments, we cannot exclude the possibility that $GABA_B$-R1/$GABA_B$-R2 heterodimers further aggregate to higher order oligomers. Our data are consistent with the notion that heteromerization of $GABA_B$-R1 and $GABA_B$-R2 is a prerequisite for the proper activation of Kir3- and GIRK-type potassium channels as well as proper posttranslational processing of $GABA_B$ receptor subunits (*6*−*11*, *16*). The finding that interactions among either $GABA_B$-R1 or $GABA_B$-R2 do not take place, can be explained by homodimer instability. Whether there is a biological significance to the instability of homotypic $GABA_B$ receptor complexes remains to be elucidated.

ACKNOWLEDGMENT

We thank Drs. C.-A. Schoenenberger and M. O. Steinmetz for helpful discussions and critical review of the manuscript. We are grateful to Dr. U. Christen for excellent technical assistance.

REFERENCES

1. Bowery, N. G. (1993) *Annu. Rev. Pharmacol. Toxicol. 33*, 109−147.
2. Mott, D. D., and Lewis, D. V. (1994) *Int. Rev. Neurobiol. 36*, 97−223.
3. Rabow, L. E., Russek, S. J., and Farb, D. H. (1995) *Synapse 21*, 189−274.
4. Bettler, B., Kaupmann, K., and Bowery, N. G. (1998) *Curr. Opin. Neurobiol. 8*, 345−350.
5. Kaupmann, K., Huggel, K., Heid, J., Flor, P. J., Bischoff, S., Mickel, S. J., McMaster, G., Angst, C., Bittiger, H., Froestl, W., and Bettler, B. (1997) *Nature 386*, 239−246.
6. Jones, K. A., Borowsky, B., Tamm, J. A., Craig, D. A., Durkin, M. M., Dai, M., Yao, W.-J., Johnson, M., Gunwaldsen, C., Huang, L.-Y., Tang, C., Shen, Q., Salon, J. A., Morse, K., Laz, T., Smith, K. E., Nagarathnam, D., Noble, S. A., Branchek, T. A., and Gerald, C. (1998) *Nature 396*, 674−679.
7. White, J. H., Wise, A., Main, M. J., Green, A., Fraser, N. J., Disney, G. H., Barnes, A. A., Emson, P., Foord, S. M., and Marshall, F. H. (1998) *Nature 396*, 679−682.
8. Kaupmann, K., Malitschek, B., Schuler, V., Heid, J., Froestl, W., Beck, P., Mosbacher, J., Bischoff, S., Kulik, A., Shigemoto, R., Karschin, A., and Bettler, B. (1998) *Nature 396*, 683−687.
9. Kuner, R., Köhr, G., Grünewald, S., Eisenhardt, G., Bach, A., and Kornau, H.-C. (1999) *Science 283*, 74−77.
10. Ng, G. Y. K., McDonald, T., Bonnert, T., Rigby, M., Heavens, R., Whiting, P., Chateauneuf, A., Coulombe, N., Kargman, S., Caskey, T., Evans, J. F., O'Neill, G. P., and Liu, Q. (1999) *Genomics 56*, 288−295.
11. Ng, G. Y. K., Clark, J., Coulombe, N., Ethier, N., Herbert, T. E., Sullivan, R., Kargman, S., Chateauneuf, A., Tsukamoto, N., McDonald, T., Whiting, P., Mezey, E., Johnson, M. P., Liu, Q., Kolakowski, Jr., L. F., Evans, J. F., Bonner, T. I., and O'Neill, G. P. (1999) *J. Biol. Chem. 274*, 7607−7610.
12. Pin, J.-P., and Duvoisin, R. (1995) *Neuropharmacology 34*, 1−26.
13. Brown, E. M., Gamba, G., Riccardi, D., Lombardi, M., Butters, R., Kifor, O., Sun, A., Hediger, M. A., Lytton, J., and Herbert, S. C. (1993) *Nature 366*, 575−580.
14. Herrada, G., and Dulac, C. (1997) *Cell 90*, 763−773.
15. Matsunami, H., and Buck, L. B. (1997) *Cell 90*, 775−784.
16. Couve, A., Filippov, A. K., Connolly, C. N., Bettler, B., Brown, D. A., and Moss, S. J. (1998) *J. Biol. Chem. 273*, 26361−26367.
17. Cohen, C., and Parry, D. A. D. (1990) *Proteins 7*, 1−15.
18. Lupas, A. (1996) *Trends Biochem. Sci. 21*, 375−382.
19. Kammerer, R. A. (1997) *Matrix Biol. 15*, 555−565.
20. Kohn, W. D., Mant, C. T., and Hodges, R. S. (1997) *J. Biol. Chem. 272*, 2583−2586.
21. Crick, F. H. C. (1953) *Acta Crystallogr. 6*, 685−689.
22. O'Shea, E. K., Klemm, J. D., Kim, P. S., and Alber, T. (1991) *Science 254*, 539−544.
23. Harbury, P. B., Zhang, T., Kim, P. S., and Alber, T. (1993) *Science 262*, 1401−1407.
24. Harbury, P. B., Kim, P. S., and Alber, T. (1994) *Nature 371*, 80−83.
25. Malaskevich, V. N., Kammerer, R. A., Efimov, V. P., Schulthess, T., and Engel, J. (1996) *Science 274*, 761−765.
26. Sodek, J., Hodges, R. S., Smillie, L. B., and Jurasek, L. (1972) *Proc. Natl. Acad. Sci. U.S.A. 69*, 3800−3804.
27. McLachlan, A. D., and Stewart, M. (1975) *J. Mol. Biol. 98*, 293−304.
28. Snead, O. C., III (1995) *Ann. Neurol. 37*, 146−157.
29. Caddick, S. J., and Hosford, D. A. (1996) *Mol. Neurobiol. 13*, 23−32.

30. Dichter, M. A. (1997) *Epilepsia 38*, S2−6.
31. Brandenberger, R., Kammerer, R. A., Engel, J., and Chiquet, M. (1996) *J. Cell Biol. 135*, 1583−1592.
32. Kammerer, R. A., Schulthess, T., Landwehr, R., Lustig, A., Fischer, D., and Engel, J. (1998) *J. Biol. Chem. 273*, 10602−10608.
33. Sambrook, J., Fritsch, E. F., and Maniatis, T. (1989) *Molecular Cloning: A Laboratory Manual*, 2nd ed.; Cold Spring Harbor Laboratory, Cold Spring Harbor, NY.
34. Edelhoch, H. (1967) *Biochemistry 6*, 1948−1954.
35. Schägger, H., and von Jagow, G. (1987) *Anal. Biochem. 166*, 368−379.
36. Chen, Y. H., Yang, J. T., and Chau, K. H. (1974) *Biochemistry 13*, 3350−3359.
37. van Holde, K. E. (1985) *Physical Biochemistry*, 2nd ed.; chapts 4 and 5, pp 93−136, Prentice Hall, Englewood Cliff, NJ.
38. Lupas, A. (1996) *Methods Enzymol. 266*, 513−525.
39. Woolfson, D. N., and Alber, T. (1995) *Protein Sci. 4*, 1596−1607.
40. Hu, J. C., O'Shea, E. K., Kim, P. S., and Sauer, R. T. (1990) *Science 250*, 1400−1403.
41. O'Shea, E. K., Rutkowski, R., Stafford, W. F., III, and Kim, P. S. (1989) *Science 245*, 646−648.
42. Muhle-Goll, C., Gibson, T., Schuck, P., Schubert, D., Nalis, D., Nilges, M., and Pastore, A. (1994) *Biochemistry 33*, 11296−11306.
43. Lavigne, P., Kondejewski, L. H., Houston, M. E., Jr., Sönnichsen, F. D., Lix, B., Sykes, B. D., Hodges, R. S., and Kay, C. M. (1995) *J. Mol. Biol. 254*, 505−520.
44. Spek, E. J., Bui, A. H., Lu, M., and Kallenbach, N. R. (1998) *Protein Sci. 7*, 2431−2437.
45. O'Shea, E. K., Rutkowski, R., and Kim, P. S. (1992) *Cell 68*, 699−708.
46. Muhle-Goll, C., Nilges, M., and Pastore, A. (1995) *Biochemistry 34*, 13554−13564.
47. Lavigne, P., Crump, M. P., Gagné, S. M., Hodges, R. S., Kay, C. M., and Sykes, B. D. (1998) *J. Mol. Biol. 281*, 165−181.
48. Gonzalez, L., Jr., Brown, R. A., Richardson, D., and Alber, T. (1996) *Nature Struct. Biol. 3*, 1002−1009.
49. Gonzalez, L., Jr., Woolfson, D. N., and Alber, T. (1996) *Nature Struct. Biol. 3*, 1011−1018.
50. Lumb, K. J., and Kim, P. S. (1995) *Biochemistry 34*, 8642−8648.
51. Cusack, S., Berthet-Colominas, C., Hartlein, M., Nassar, N., and Leberman, R. (1990) *Nature 347*, 249−255.
52. Lavigne, P., Sönnichsen, F. D., Kay, C. M., and Hodges, R. S. (1996) *Science 271*, 1136−1137.
53. Lumb, K. J., and Kim, P. S. (1996) *Science 271*, 1137−1138.
54. Krylov, D., Barchi, J., and Vinson, C. (1998) *J. Mol. Biol. 279*, 959−972.
55. Dames, S. A., Kammerer, R. A., Moskau, D., Engel, J., and Alexandrescu, A. T. (1999) *FEBS Lett. 446*, 75−80.

BI991018T